Trade-off between redox potential and strength of electrochemical CO_2 capture in quinones

Anna T. Bui, Niamh A. Hartley, Alex J. W. Thom*, and Alexander C. Forse*

Yusuf Hamied Department of Chemistry, University of Cambridge, Lensfield Road, Cambridge, CB2 1EW, United Kingdom

Electrochemical carbon dioxide capture has recently emerged as a promising alternative approach to conventional energy-intensive carbon capture methods. The most common electrochemical capture approach is to employ redox-active molecules such as quinones. Upon electrochemical reduction, quinones become activated for the chemical capture of CO_2. The main disadvantage of this method is the possibility of side-reactions with oxygen, which is present in almost all gas mixtures of interest for carbon capture. This issue can potentially be mitigated by fine-tuning redox potentials through the introduction of electron-withdrawing groups on the quinone ring. In this article, we investigate the thermodynamics of the electron transfer and chemical steps of CO_2 capture in different anthraquinone derivatives with a range of substituents. By combining density functional theory calculations and cyclic voltammetry experiments, we discover a trade-off between redox potentials and the strength of CO_2 capture. We show that redox potentials can readily be tuned to more positive values to impart stability to oxygen, but as a consequence, significant decreases in CO_2 binding free energies are observed. This trade-off must be taken into consideration for the design of improved redox-active molecules for electrochemical CO_2 capture.

I. INTRODUCTION

Anthropogenic carbon dioxide (CO_2) emission is the major contribution to global climate change,[1] presenting an urgent challenge to our society.[2,3] One of the many important mitigation strategies for reducing greenhouse gas emissions is carbon capture. Conventional carbon capture technology involves wet chemical scrubbing using aqueous amines to absorb CO_2 at industrial sources or directly from the air for further sequestration.[4] This strategy, however, has many limitations including low capacities, poor oxidative stability, degradation in presence of contaminants and large thermal energy demand for absorbent regeneration.[4–6] In the search for new materials and technologies for carbon capture, electrochemically mediated CO_2 capture has emerged as a promising approach.[7–10] A popular strategy is to use redox-active organic compounds as CO_2 carriers, with quinones being the most representative class of compounds. Electrochemical reduction of quinones generates oxyanion nucleophiles, which have high binding affinities towards CO_2 and have been reported to concentrate and selectively separate CO_2.[11–15] The biggest advantage is that quinones can be electrochemically regenerated, leading to energy savings over traditional temperature or pressure swing processes.

While the recently reported use of quinone-functionalised electrodes is promising,[16] questions remain about the molecular mechanism of this process and whether it is possible to increase its oxidative stability by carefully tuning the electron density of the quinones. In the presence of oxygen (O_2), it is observed that there is a loss in CO_2 capture ability[16] as reduced quinones can be re-oxidised while O_2 is reduced.[17] If quinone structures are tuned to have sufficiently positive reduction potentials by substitution of functional groups

on the aromatic rings, it may be possible to avoid the side-reactions with O_2. However, by tuning the redox potentials, one might also change the CO_2 capturing ability of the quinones. While this has been hinted at by cyclic voltammetry (CV) studies of different quinone derivatives under CO_2,[18,19] a complete assessment of the relationship between redox potentials and CO_2 capturing abilities has not been carried out. We believe this is because (i) quantifying the thermodynamic driving force of CO_2 capture through CV alone is challenging and (ii) a systematic electrochemical study of quinone derivatives with different number of substituents and different functional groups is not easily accessible experimentally.

Both of these challenges can be tackled computationally through quantum chemical calculations. As quinones and their derivatives are also of interest in energy storage applications, several studies have computationally examined their redox properties, including the effect of electron-donating groups (EDGs) and electron-withdrawing groups (EWGs),[20,21] substituent pattern effects[22] and their structure-property relationships.[23] Most of these works are based on density functional theory (DFT), which has proven to be an affordable and reliable way to study redox properties of organic molecules.[24,25] It is worth emphasising that these previous studies, however, did not examine electrochemical CO_2 capture.

In this article, we provide a detailed assessment of the relationship between redox potentials and CO_2 capturing abilities of different anthraquinone (AQ) derivatives. This is done both experimentally with CV and computationally with DFT calculations of the Gibbs free energy change upon CO_2 capture. Our results uncover a trade-off between the redox potential and the strength of CO_2 capture, which is seen by fine-tuning the electron density on the quinone rings. This trade-off has important impli-
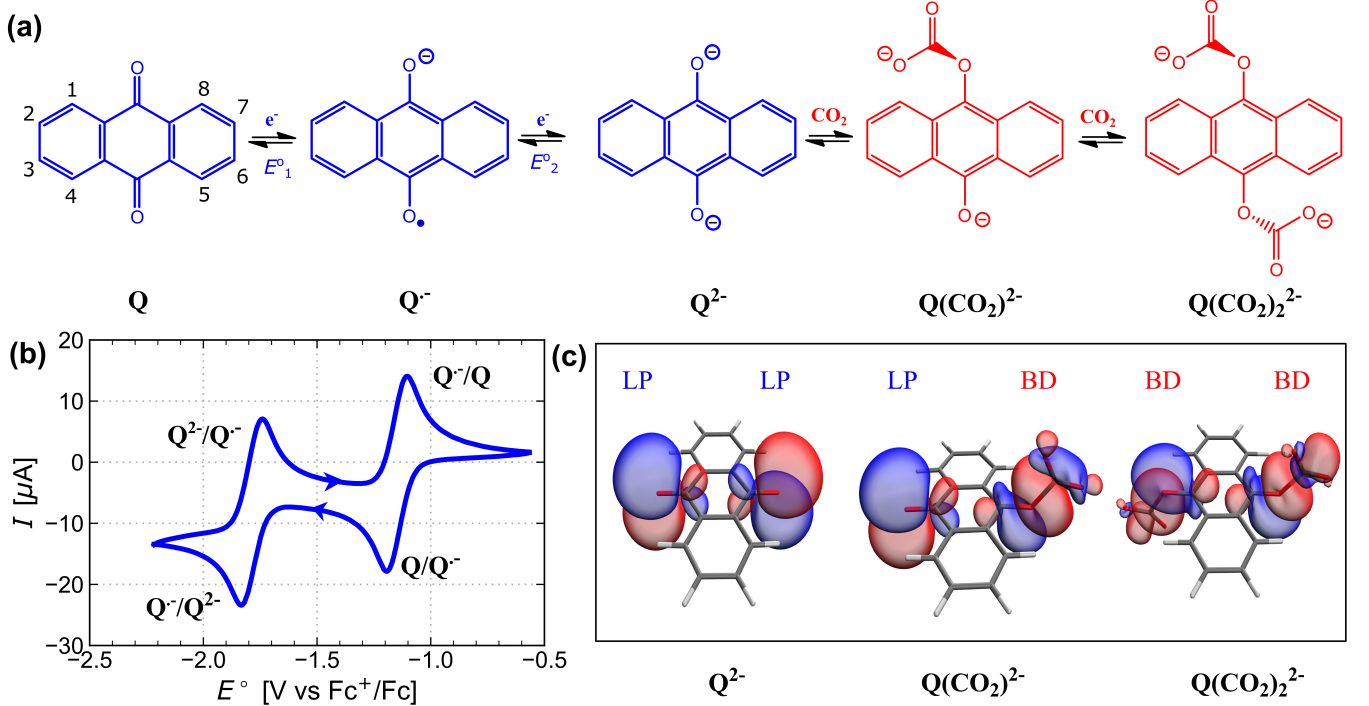
Figure 1. The EECC reaction scheme of electrochemical CO_2 capture by AQ. (a) The stepwise EECC reaction scheme employed in our DFT calculations includes two electron transfer steps followed by two chemical steps. (b) Experimental CV of AQ in DMSO under N_2 with cathodic and anodic peaks labelled with ox/red species at a scan rate of $10\,\mathrm{mV\,s^{-1}}$. (c) Orbitals representing the nucleophilic lone pairs (LP) and the O-CO_2 bond (BD) formed from NBO analysis of DFT results.

cations in raising the efficiency of future electrochemical CO_2 capture technologies.

II. RESULTS AND DISCUSSION

Reaction scheme and the oxyanion nucleophilicity

In this work we describe the overall quinone-mediated electrochemical CO_2 capture process by an "EECC" reaction scheme. In this mechanism, two electron transfer (E) steps occur first according to Figure 1(a):

$$Q + e^- \rightarrow Q^{\bullet-}, \tag{1}$$

$$Q^{\bullet-} + e^- \rightarrow Q^{2-}, \tag{2}$$
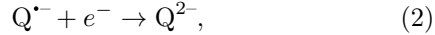
where Q is the neutral quinone, $Q^{\bullet-}$ is the semiquinone radical anion, and Q^{2-} is the quinone dianion. In the absence of CO_2, the CV of anthraquinone in DMSO exhibited the expected two reduction waves corresponding to processes (1) and (2) at potentials of $E_1^\circ = -1.3\,\mathrm{V}$ and $E_2^\circ = -2.0\,\mathrm{V}$ vs $\mathrm{Fc^+/Fc}$, respectively, where mid-point potentials have been used (Figure 1(b)).

In the EECC scheme, it is assumed that the two electrochemical steps (E) are followed by two chemical (C) steps according to Figure 1(a):

$$Q^{2-} + CO_2 \rightarrow Q(CO_2)^{2-}, \tag{3}$$

$$Q(CO_2)^{2-} + CO_2 \rightarrow Q(CO_2)_2^{2-}, \tag{4}$$
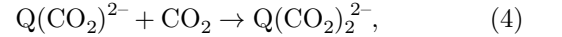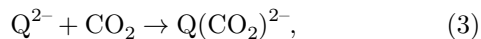
where $Q(CO_2)^{2-}$ is the monocarbonate dianion and $Q(CO_2)_2^{2-}$ is the dicarbonate dianion.

We employ this mechanism in our analysis for two reasons: (i) the EECC mechanism has been supported in previous CV analysis of EWG-substituted quinones at low CO_2 concentration.[16,19,26,27] Since our goal is to mitigate side-reactions of reduced quinones with O_2, our main interest is to add EWGs to stabilise the reduced quinones, increasing the likelihood of both electrochemical reduction steps being required prior to CO_2 capture; (ii) this scheme also allows the combination of two reduction steps (1) and (2) to an "EE" step, and two capturing events (3) and (4) to a "CC" step according to:

$$Q + 2e^- \rightarrow Q^{2-}, \tag{5}$$

$$Q^{2-} + 2CO_2 \rightarrow Q(CO_2)_2^{2-}. \tag{6}$$
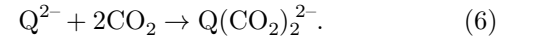
This is not only convenient for the calculation of the Gibbs free energy ($\Delta G_{\mathrm{CC}}^\circ$) upon CO_2 capture but the combined two-electron reduction potential (E_{EE}°) from DFT is also more accurate than the separate one-electron reduction potentials (E_1° and E_2°), as detailed in the next section. We note that other electrochemical capture mechanisms are possible, notably the ECEC mechanism, where after the first reduction step, $Q^{\bullet-}$ reacts with

Species	C-O quinone/ Å	O$-$CO$_2$/ Å
Q	1.220	-
Q$^{\bullet-}$	1.257	-
Q^{2-}	1.291	-
Q(CO$_2$)$^{2-}$	1.269 / 1.380	1.495
Q(CO$_2$)$_2^{2-}$	1.356	1.553

Table I. C-O bond lengths from DFT calculations. For Q(CO$_2$)$^{2-}$, the values are given for C-O bond of the quinone on the side where CO$_2$ is not bound and is bound respectively.

CO$_2$ to form the semicarbonate anion Q(CO$_2$)$^{\bullet-}$, as suggested in studies of EDG-substituted quinones at high CO$_2$ concentration.[14,15,19,26]

We first explored the CO$_2$ capture steps for anthraquinone using DFT calculations. The localised orbital forms representing the lone pairs (LPs) and two-electron two-centre bonds (BDs) were decomposed from the DFT wavefunction by natural bonding orbital analysis (NBO) (Figure 1(c)).[28] Upon reduction the quinone C-O bond length increases (Table I), and NBO analysis shows a change from C-O π orbital in Q to a lone pair on O in Q^{2-} (SI), which is consistent with the canonical Lewis structures. For each carbon capture event, a LP on an oxygen acts as a nucleophile and attacks a CO$_2$ molecule, forming a C-O BD to CO$_2$ (Figure 1(c)). It is clear that this oxygen LP and its electron density governs the nucleophilicity of Q^{2-} and its CO$_2$ capture ability. Upon the second carbon capture event, the bond length of O-CO$_2$ decreases and the quinone C-O bond length increases (Table I), suggesting a decrease in bonding affinity towards CO$_2$. This is consistent with the carbonate group withdrawing electron density from the initially free oxyanion centre.

Benchmarking reduction potentials of substituted anthraquinones from CV and DFT

Before proceeding to look at the effect of quinone functionalisation on electrochemical CO$_2$ capture, we compared the computed and experimental CV redox potentials for selected AQ derivatives to evaluate the reliability of DFT calculations. Figure 2(a) shows their structures and Figure 2(b) shows the corresponding CVs in DMSO under N$_2$. The mid-point potentials of the pair of redox peaks in CV are taken as single reduction potentials E_1° and E_2°. The average of E_1° and E_2° is then taken as the double reduction potential E_{EE}°. The corresponding values calculated from DFT (detailed in the Methods section) are compared to experimental single and double reduction potentials, as shown in Figures 2(c) and 2(d), respectively.

In all cases, E_1° is more positive than E_2° as it is easier to reduce Q than Q$^{\bullet-}$. This is because (i) the gain of an electron is more favourable for neutral Q than for negatively charged Q$^{\bullet-}$ on electrostatic grounds and (ii) there is a greater contribution from solvation to the reduction

driving force for the second than the first reduction (Figure S4).

When EWGs are substituted, as in the case of -Cl and -F, the reduction potentials become more positive for both CV and DFT results (Figures 2(c), 2(d)). This agrees with previous studies[19,20,23] and is consistent with the electron density on the reduced quinones being more delocalised, making reduction more thermodynamically favourable. Positional effects observed experimentally and predicted computationally for the case of -Cl also agree: substitution at the 2- position shifts E_{EE}° to a more positive value than at the 1- position. This is consistent with greater delocalisation of electron density when Cl is substituted at the 2- position with a larger LUMO coefficient in Q (Figure S1). The largest shift of 0.4 V due to multiple substitution in the case of octafluoroanthraquinone AQ-F$_8$ is also well predicted by DFT.

When EDGs are substituted, as in the case of -OMe, the reduction potentials become more negative for both CV and DFT results as the reduced forms become disfavoured. In the case of -OH, however, intramolecular hydrogen-bonding stabilises the Q^{2-} form so an overall increase in E_{EE}° is observed. This is supported by the change in DFT geometry: the hydroxyl proton in Q transfers to quinone O following electrochemical reduction (Figure S2).

While the computed E_{EE}° values generally compare favourably with experimental measurements, with error less than 0.05 V, there are greater deviations in trend for E_1° and E_2°. We believe this due to a well-known problem of DFT in describing certain radical anions of atoms and small molecules.[29–32] Treating EE as a single two-electron reduction step (5) allows the radical semiquinone anion Q$^{\bullet-}$ to be bypassed, the accurate treatment of which calls for a higher level of theory. Overall, the good agreement between computed and experimental E_{EE}° values provided validation of the DFT approach to study electrochemical reduction of quinones and enabled us to explore a wider range of functional group substitutions in the next section.

Effect of tuning quinone electron density on electrochemical CO$_2$ capture thermodynamics

We now explore how varying the electron density of quinones impacts electrochemical CO$_2$ capture through a F-substituted AQ series. F is a good candidate to be used for fine-tuning because (i) F substituents tend to show a strong negative inductive effect of an EWG that predominates the positive resonance effect of an EDG,[22] (ii) there are various ways to fluorinate AQ selectively[33–35] and (iii) the small size of F minimises steric effects, whereas the large substituents can decrease the CO$_2$ capturing ability, as previously observed in Cl-substituted quinones.[27]

The thermodynamics governing the EE and CC steps for AQ derivatives with increasing number of F-substituents are now quantified from DFT calculations.
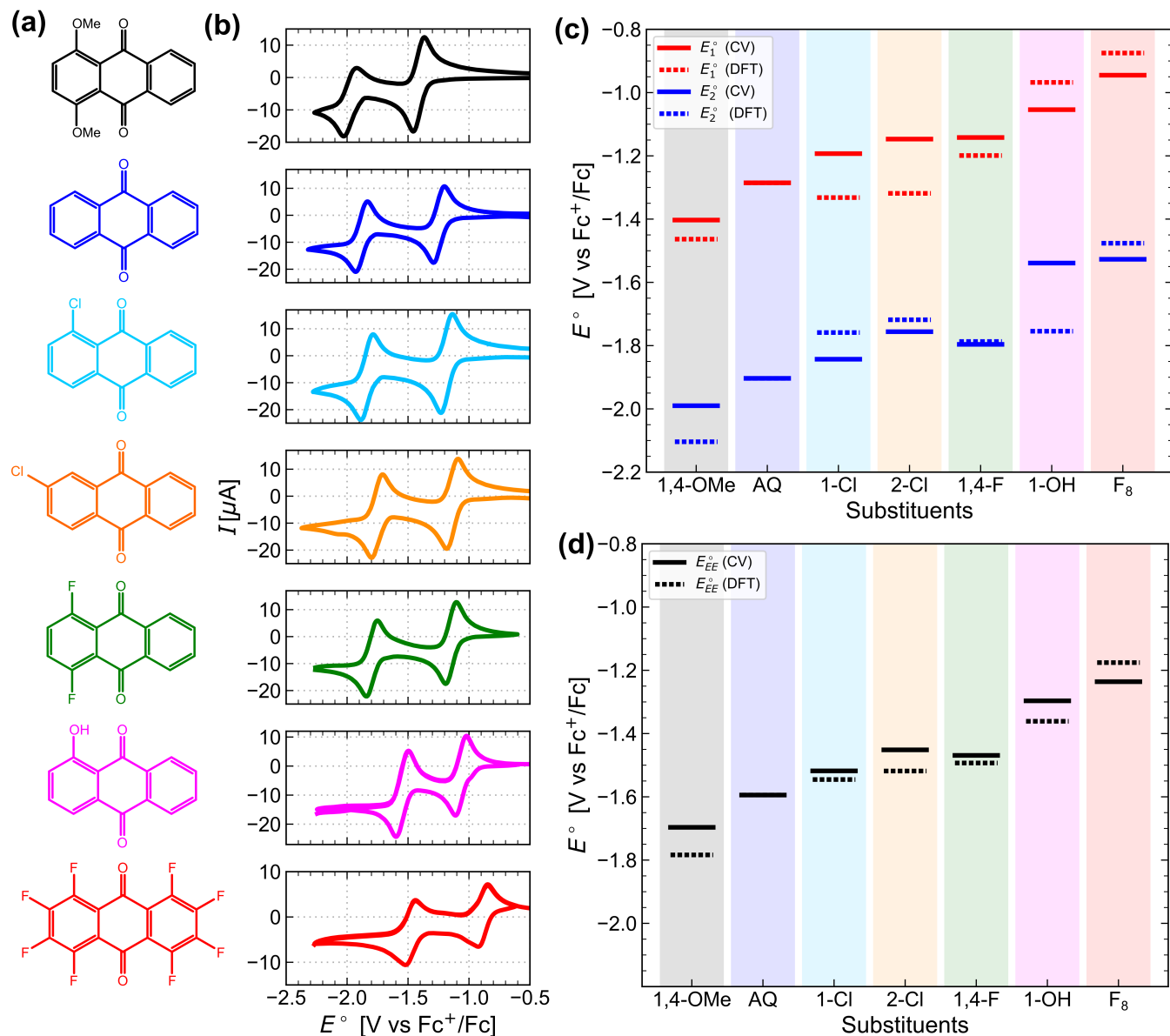
Figure 2. Reduction potentials of selected AQ derivatives. (a) Structure of all selected compounds. (b) CVs of AQ derivatives under N_2 in DMSO at a scan rate of $10\,\mathrm{mV\,s^{-1}}$. (c) Comparison of single reduction potentials from CV and DFT. (d) Comparison of double reduction potentials from CV and DFT. DFT reduction potentials are calculated as reference to AQ.

Figure 3(a) shows that the computed E°_{EE} increases from $-1.54\,\mathrm{V}$ to $-1.17\,\mathrm{V}$ against $\mathrm{Fc^+/Fc}$ upon substitution of one to eight F, and is generally directly proportional to the number of F substitutions made. As more electron density is withdrawn from the oxygens in the $\mathrm{Q^{2-}}$ anion, the reduced form is more delocalised and stabilised against re-oxidation. The increase in reduction potential varies slightly for different positions of substitutions for F, as seen previously in the case of other substituents.[20–22] When EDGs are substituted instead, the opposite effect is seen (Figure S3). Overall, increasing the number of F substitutions leads to approximately linear increase in the reduction potentials of AQ. In the

context of electrochemical CO_2 capture, the EE step (5) is more thermodynamically favourable as electron density of quinones are tuned with increasing number of EWGs, which should impart improved stability in oxygen.

We then evaluated the thermodynamics of the chemical CO_2 capture steps for our F-substituted AQ series (Figure 3(b)). The computed Gibbs free energy change $\Delta G^\circ_{\mathrm{CC}}$ increases by $40\,\mathrm{kJ\,mol^{-1}}$ upon substitution of one to eight F. Again, the effect is approximately linear, and there is no consistent trend in position of substitution. This effect can be explained by considering the electron density available in $\mathrm{Q^{2-}}$ for bonding with CO_2 to form $\mathrm{Q(CO_2)_2^{2-}}$. AQ-F_8 has a lower charge density on the oxy-
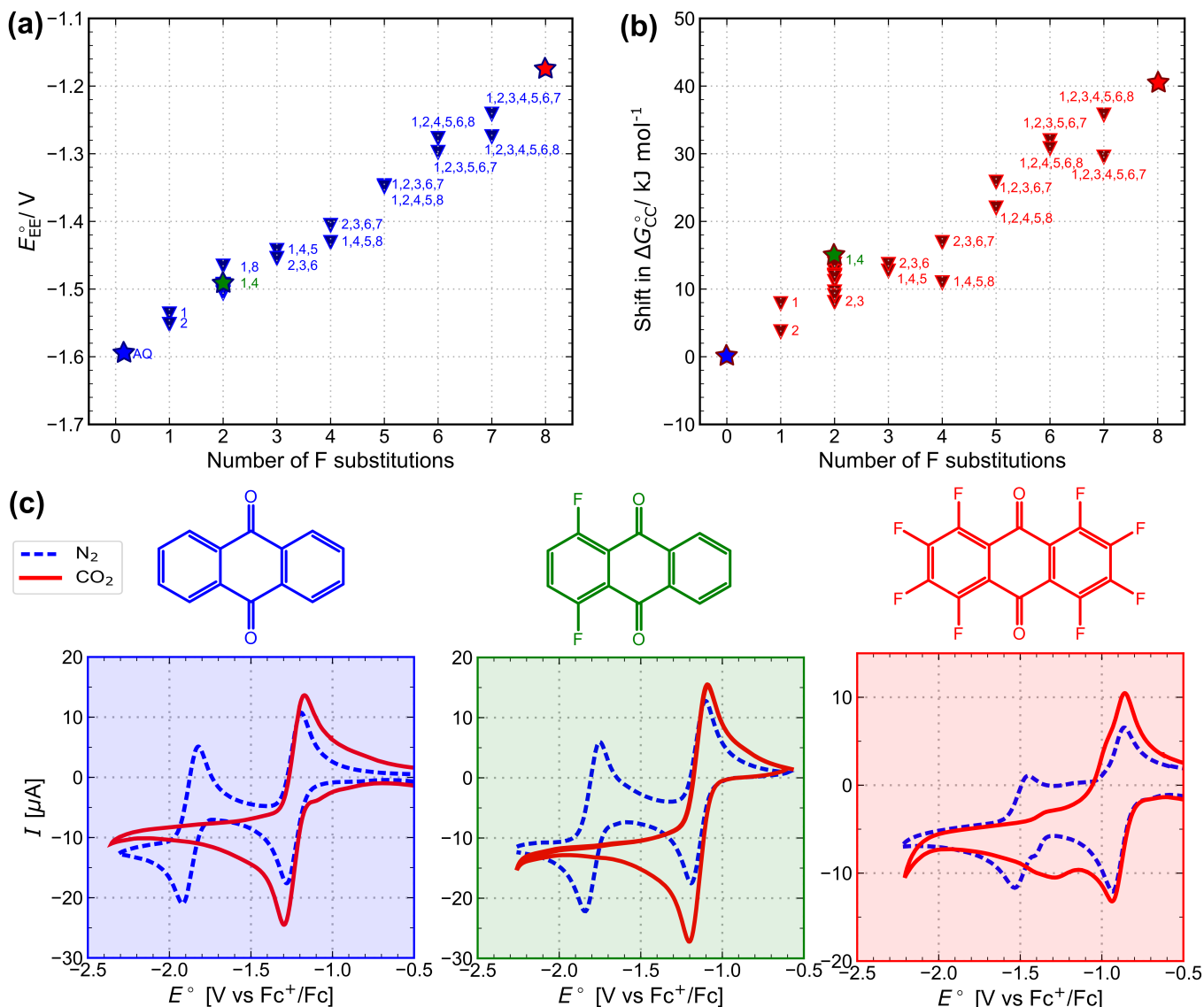
Figure 3. Calculated reduction potential and capturing ability for F-substituted AQ derivatives. (a) Variation in the reduction potential for two-electron reduction. (b) Variation in the Gibbs free energy changes for double CO_2 capture relative to AQ. (c) Experimental CVs of unsubstituted AQ, 1,4-F-AQ and AQ-F$_8$ (given starred symbols in (a) and (b)) under N$_2$ and under CO_2 at a scan rate of $10\,\mathrm{mV\,s^{-1}}$.

gen than unsubstituted AQ in its Q^{2-} form and therefore has a lower affinity for binding to CO_2. The O$-CO_2$ bond length of the Q(CO$_2$)$_2^{2-}$ form is 1.676 Å in AQ-F$_8$ compared to 1.553 Å in AQ, indicating a weaker bond being formed due to more electron density being delocalised away from the oxygens in Q^{2-}. Overall, increasing the number of F substitutions leads to approximately linear increase in the Gibbs free energy change in the chemical reaction with CO_2. In the context of electrochemical CO_2 capture, the CC step (6) is less thermodynamically favourable as electron density of quinones are tuned with increasing number of EWGs, suggesting a trade-off between redox potential and CO_2 affinity.

To explore this result experimentally, we measured the

CVs of unsubstituted AQ, 1,4-F-AQ and AQ-F$_8$ under N$_2$ and under CO_2 (Figure 3(c)). For all cases, the reduction wave positions of the first electron transfer (1) remain unchanged in the presence and absence of CO_2. This is in line with the quinone in all cases needing to be first activated by reduction before capturing CO_2, as observed in previous studies.[19] For both AQ and 1,4-F-AQ, the second reduction wave (2) appears to shift underneath the first reduction wave, in agreement with previous work.[14,16] In contrast, for AQ-F$_8$ a smaller shift of the first reduction wave is observed, and two redox processes can be clearly observed under CO_2. The smaller positive shift of the second reduction peak for AQ-F$_8$ indicates less stabilisation of the reduced species by CO_2 than for

AQ and 1,4-F-AQ, and suggests a smaller binding constant to CO_2,[19] as predicted by our DFT calculations. The reduction in height of the second reduction wave for AQ-F_8 is an indication of some reactivity with CO_2, to form either $Q(CO_2)^{2-}$ or $Q(CO_2)_2^{2-}$ species.[15] Overall, these experimental results are consistent with the predictions of our DFT calculations, providing support for the calculated trade-off between redox potential and CO_2 capture strength.

Trade-off between redox potential and strength of CO_2 capture

The above results indicate that by adding electron withdrawing groups we are simultaneously making electrochemical reduction more favourable and carbon capture less favourable. This implies that when designing quinone derivatives for electrochemical CO_2 capture to enhance efficiency, a balance between favouring electron transfer and chemical steps must be taken into account. For the F-substituted AQ series, this trade-off can be seen clearly by combining Figures 3(b) and 3(c) into a plot of the shift in ΔG°_{CC} against the shift in E°_{EE}, as shown in 4(a). The shifts are relative to the unsubstituted AQ and regions where each step is favoured or disfavoured are colour-coded accordingly. The linear trend that emerges confirms the unfavourable relationship between the thermodynamics of cathodic activation and nucleophilic addition of CO_2.

After demonstrating this trade-off for the F-substituted AQ series, we posed the question of whether it is possible to overcome this trade-off by using other functional groups. i.e. can we favour the EE step without disfavouring the CC step significantly, thereby falling below the linear fit (blue lines in Figures 4(a) and 4(b)). We therefore explored a range of mono-substituted AQ derivatives with different functional groups (Figure 4(b)), including -F, -Cl, -Br and -CF_3 as halogen-based EWGs, -C_2H_3 (ethylene), -COOMe and -CN as resonance-based EWGs and -CH_3, -OMe and -NMe_2 as EDGs. Indices 1- and 2- indicate the positions of substitution[36], and the plot is again colour-coded according to how the thermodynamics of cathodic activation and nucleophilic addition are changed from that of unsubstituted AQ. The unfavourable relationship still remains: substitution of EWGs favours the EE step but disfavours the CC step while substitution of EDGs favours the CC steps but disfavours the EE steps. For most substituents, substitution closer to the carbonyl group at position 1- leads to a higher ΔG°_{CC} due to steric hindrance between the captured CO_2 and the substituents. The tuning window of these single substitutions is approximately 0.5 V for E°_{EE} and 50 kJ mol^{-1} for ΔG°_{CC}. Although these mono-substituted derivatives do not all fall on the same linear fit for the F-substituted AQ series, the deviation from the trend is small and it would be very difficult to fine-tune the electron density of AQ using these functional

groups to favour both the EE and CC steps. It is useful to tie these results back to the role of the electron density in the oxyanion Q^{2-}. Delocalisation of the electron density around the ring would stabilise the quinone in its dianion Q^{2-} form. This would mean it is less likely to be re-oxidised by O_2 after being electrochemically reduced, but also less likely to have good nucleophilicity to react with CO_2.

A further avenue to break the observed trade-off could be to explore alternative capture agents beyond anthraquinone. Our calculations on substituted benzoquinones (BQ) also revealed a trade-off between redox potential and CO_2 capture strength (Figure S5), though interestingly we found that both the reduction and carbon capture steps become more thermodynamically favourable relative to AQ (Figure S5). The downsides of BQ, however, are that its fine-tuning ability is limited by the total number of possible substitutions, and BQs are also more electrochemically unstable and susceptible to side reactions and degradation.[37] Other redox active molecules, such as naphthoquinones, therefore, might be able to provide a better compromise and are worth investigating in future work.

Overall, we have demonstrated that the trade-off between redox potential and strength of electrochemical CO_2 capture is general to the fine-tuning of quinones by functional group substitutions through (i) different numbers of substituents and (ii) different types of substituents. This raises questions about whether functional group substitutions can be used to address oxygen sensitivity issues in these systems, while maintaining sufficient CO_2 reactivity.

To assess the impact of oxygen, the CV of unsubstituted AQ under O_2 in DMSO was measured, which showed weak quinone oxidation waves (Figure S6), indicating reactivity with O_2. To avoid the possibility of parasitic reactions after cathodic activation, intuitively one would select a quinone with EWGs and a more positive reduction potential, assuming that the reduction potential is both a measure of how likely reduced quinone get re-oxidised by oxygen or chemically react with an electrochemically reduced oxygen species. However, as we shown through DFT, the reactivity of the quinone to CO_2 is weaker (main implication of the trade-off) and through CV experiments, the form of the CV is changed with a smaller positive shift of the second reduction peak. Therefore, just naively adding EWGs not only reduces CO_2 capture ability but also does not necessarily solve the O_2 reactivity problem. To this end, we provide some rough guidelines for fine-tuning to optimise the efficiency of quinone-mediated electrochemical CO_2 capture in DMSO:

(i) Unsubstituted AQ shows reactivity with O_2 so some sort of substitution is likely to be necessary.

(ii) Substitutions of bulky groups are undesirable based on steric grounds.
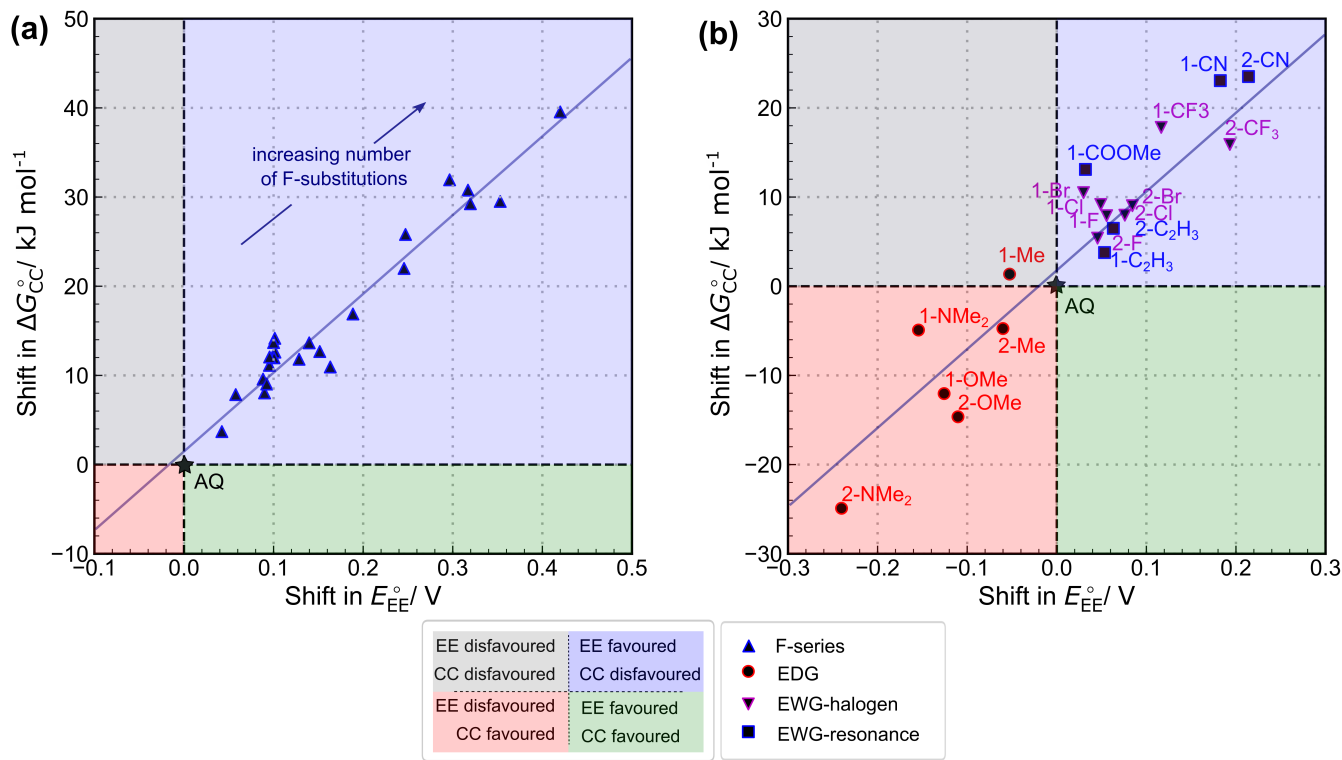
(iii) Substitutions at the 2- position create less steric

Figure 4. Trade-off between redox potential and strength of CO_2 capture. The computed shift in Gibbs free energy change for the CC steps is plotted against the shift in 2-electron reduction potential EE in DMSO computed for (a) multiple F-substituted AQ derivatives and (b) the mono-subsituted AQ derivatives. The blue line is the best fit for the F-series.

hindrance for CO_2 capture than at the 1- positions, and so are advantageous for tuning the redox potentials while maintaining CO_2 reactivity.

(iv) A combination of different functional groups for multiple substitutions might be necessary, i.e EDGs at certain positions and EWGs at others, to avoid the trade-off.

These guidelines are admittedly crude, relying on the assumptions that reaction with CO_2 proceeds through an EECC mechanism and the half-wave potential of O_2 does not change in the presence of quinone species. Moreover, other factors including but not limited to CO_2 concentration, temperature, electrolyte concentrations and solvents are likely to affect the desired properties of the quinones. Incorporation of these factors goes beyond the scope of the present article and these guidelines and therefore await full validation by explicit experiments and calculations in the presence of O_2. However, the finding of this trade-off between the redox potential and the strength of CO_2 capture can be easily generalised and the discussion presented is of value for the design of improved redox active molecules for electrochemical carbon dioxide capture.

III. SUMMARY AND OUTLOOK

In this article, we have investigated the effect of fine-tuning the electron density in quinones through functional group substitution on the thermodynamics of electrochemical CO_2 capture. Specifically, we have adopted an EECC scheme to describe the overall capture process and identified the electron density of the oxyanion Q^{2-} species as the key factor governing the thermodynamics of the EE and CC steps. After benchmarking DFT calculation of the electrode potentials to CV values, we quantified the thermodynamic driving force of the EE and CC steps by the two-electron reduction potential $E°_{EE}$ and the Gibbs free energy change upon double CO_2 capture $\Delta G°_{CC}$, respectively. The electron density in AQ can be fine-tuned through the control of the number of substitutions made on the aromatic rings and the type of functional groups substituted. With both types of tuning, we have found that there is a trade-off between the redox potential and strength of electrochemical CO_2 capture in quinones. The weaker CO_2 binding manifests in a less positive shift of the second reduction peak under CO_2 for EWG substitution. We demonstrated that there is a need to fine-tune the quinones such that the EE steps are favoured (so side-reactions with O_2 are disfavoured) without disfavouring the CC steps significantly.

The combination of CV experiments and DFT calculations in studying quinone-mediated CO_2 capture not only facilitates verification of experimental observations and accurate prediction of thermodynamic quantities but also sheds light on the tuning ability, redox window and elementary steps of a reaction. These are complementary experimental and computational methods for electrochemical processes because CV can provide useful insights on electron transfer steps while DFT can investigate chemical steps in detail. While we have focused on AQ derivatives in DMSO, the method employed can be extended to other quinones with similar capturing behaviours like BQ (Figure S5),[18] NQ[13] or quinacridone.[12] Effects of other aprotic solvents can be easily extended with the current method using implicit solvation models while those of ionic liquids in recent developments[13,14] are likely to call for combination with more expensive hybrid quantum mechanics/molecular mechanics approach. Not only limited to quinones, such studies would be appropriate for other redox-active carriers that can form adducts with CO_2 such as reduced sulphides.[38]

The trade-off between redox potential and strength of CO_2 capture has important implications in electrochemical carbon capture process. As the unfavourable relationship comes from the inherent role of the electron density on the nucleophile, we hope to motivate novel ways to work around this trade-off in the rational design of new CO_2 capture materials. Of particular relevance to this work is the recent study by Simeon et al.,[19] suggesting that quinones with EDG substitutions are more suitable candidates for capturing CO_2 without side reactions with O_2. It was proposed that these undergo a ECEC scheme and this was attributed to the disappearance of the second reduction wave in their CVs. Combining these CV analyses with the approach we employ using DFT, one can investigate the thermodynamics of different potential capture mechanisms and see if such a trade-off still persists. We also note that very recent work has shown that electrolyte additives such as alcohols offer another interesting means to tune electrochemical CO_2 capture thermodynamics,[39] and it will be interesting to explore the trade-off between redox potential and capture strength with that approach. Overall, our work reveals the trade-off between redox potential and the strength of electrochemical CO_2 capture, and provides a foundation for the design of improved molecules and materials that can mitigate greenhouse gas emissions.

IV. METHODS

Experimental section

Materials: Anthraquinone (AQ, 97%), octafluoroanthraquinone (AQ-F_8, 96%), 1,4-methoxyanthraquinone (1,4-OMe-AQ, > 99%), 1,4-difluoroanthraquinone (1,4-F-AQ, 98%), ferrocene (Fc), tetrabutylammonium hexafluorophosphate (TBAPF$_6$) were purchased from Sigma Aldrich. 1-Chloroanthraquinone (1-Cl-AQ, 98%) was purchased from Thermo Scientific Chemicals. 2-Chloroanthraquinone (2-Cl-AQ, > 99%) was purchased from Chemcruz Enterprises LTD. 1-hydroxyanthraquinone (1-OH-AQ, > 95%) was purchased from Cayman Chemical Company. Dimethyl sulfoxide (DMSO) was purchased from Thermo Fisher Scientific. All chemicals were used without further purification.

Electrochemical experiments: Cyclic voltammetry measurements were carried out with a standard three-electrode cell using a BioLogic Sp-150 with BioLogic EC-Lab software. Electrochemical measurements were conducted in a glass cell. The glassy carbon working electrode, platinum wire counter electrode and leak-free Ag/AgCl reference electrode were all purchased from Alvatek. 5 mM Fc was used as the internal standard after the measurements were taken. Tetrabutylammonium hexafluorophosphate in DMSO (0.1 M) was used as the electrolyte. 1 mM of quinone was stirred in electrolyte before gas purging. The solution was purged under N_2 for 2 hours, while stirring. For electrochemical tests with quinones under CO_2, the electrolyte was bubbled with 100% CO_2 for 2 hours before experiments were run. All the measurements were recorded at a scan rate of $10\,\mathrm{mV\,s^{-1}}$.

Computational section

DFT calculations, vibrational analysis were performed in Q-Chem 5.3.[40]

Thermodynamic quantities were calculated for the combined EE and CC steps shown in Equations (5) and (6) for the EECC mechanism. For each AQ derivative involved, the gas-phase geometry was optimised at the B3LYP/6-311++G** level[41–44] and thermodynamic quantities were calculated at $T = 298.15\,\mathrm{K}$ and $P = 1\,\mathrm{atm}$. SCF calculations were considered to have converged when the wavefunction DIIS error was less than 10^{-11}. At the end of each successful geometry optimisation, the structure was checked to be a real minimum on the potential energy surface and thermodynamic corrections were obtained by vibrational frequency analysis.

The SMD implicit solvation model[45] has been reported to agree well with experimental data for computation of reduction potentials of quinone derivatives.[20] Using the optimised gas-phase geometries, single-point energy calculations were performed using the SMD model using dimethylsulfoxide (DMSO) as the solvent. Gas-phase geometries were considered throughout to eliminate dependency on solvent model and this can be justified as there is almost no significant change in geometry upon optimisation in an implicit solvation model. Previously, it has also been shown that for quinones, there is no real added value of performing geometry optimisations with implicit solvation, not to mention that they are also computationally more demanding.[25]

The reduction potentials for the electron transfer steps are calculated by considering the half-reaction

$$Q + ne^- \rightarrow Q^{n-}. \tag{7}$$

For an n-electron reduction of quinones in solvent, the absolute reduction potential of the half reaction is given by the Nernst equation:

$$E^\circ_{\text{abs}} = -\Delta G^\circ_{\text{rxn}}/nF \tag{8}$$

where G°_{rxn} is the standard Gibbs free energy per coulomb of charge transferred during the reaction, n is the number of electrons and F is the Faraday constant. The Gibbs free energy of a redox species in solution is given by

$$G^\circ = U_{\text{gas}} + E_{0,\text{gas}} + H_{\text{gas}} - TS_{\text{gas}} + F_{\text{solv}} \tag{9}$$

where U_{gas} denotes the Born-Oppenheimer equilibrium potential energy, $E_{0,\text{gas}}$ denotes the vibrational zero point energy, H denotes the enthalpic contribution, TS_{gas} denotes the entropic contribution to the Gibbs free energy with $T = 298.15\,\text{K}$ in gas phase and F_{solv} denotes the solvation free energy from the solvation model. *Ab initio* calculations of reduction potentials using the thermodynamic cycle have been covered in more details elsewhere.[46] Since experimental reduction potentials are measured relative to a reference electrode potential, theoretical calculations are typically carried out for a half-cell reaction with the substraction of a reference electrode. The *ab initio* E° might agree quantitatively with the experimental value; however the two are not directly equivalent due to cell resistance, concentration dependence or a lack of better solvation treatment in calculations.[47,48] Therefore, the potentials were calculated relative to those of a reference compound, rather than as absolute potentials, in order to remove the influence of systematic errors between the experimental conditions used here and those used to determine absolute potentials of reference compounds reported elsewhere. AQ was chosen as the reference compound and isodesmic reaction schemes for the reduction and oxidation of are given as follows:

$$AQ^{2-} + Q \rightarrow AQ + Q^{2-} \tag{10}$$
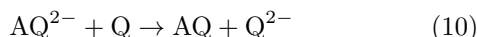
Using the $\Delta G^\circ_{\text{rxn}} = -nFE^\circ_{\text{rxn}}$ relationship:

$$E^\circ(Q/Q^{2-}) = \Delta G^\circ_{\text{rxn}}/nF - E^\circ_{\text{exp}}(AQ/AQ^{2-}) \tag{11}$$

For the EECC mechanism, the electron transfer EE steps are considered as a single two-electron reduction and the calculated E° values are given in reference to Fc^+/Fc. For the chemical steps CC, the standard Gibbs free energies are given.

SUPPLEMENTARY INFORMATION

Supplementary information includes: Orbital analysis of species in EECC for AQ, Hydrogen bonding in OH case, Substitutions of Me-series, Going from gas phase to solution phase, Trade-off in BQ F series, CV of AQ under O_2.

DATA AVAILABILITY STATEMENT

The data that supports the findings of this study, optimised geometries of compounds for the DFT calculations and scripts to calculate reduction potentials and Gibbs free energies will be openly available at the University of Cambridge Data Repository.

REFERENCES

[1] R. K. Pachauri and L. Meyer, "Climate change 2014: Synthesis report. Contribution of working groups I, II and III to the fifth assessment report of the Intergovernmental Panel on Climate Change," IPCC report (2015).

[2] J. Tollefson and K. R. Weiss, "Nations approve historic global climate accord," Nature **528**, 315–316 (2015).

[3] W. Cai, A. Santoso, G. Wang, S.-W. Yeh, S.-I. An, K. M. Cobb, M. Collins, E. Guilyardi, F.-F. Jin, J.-S. Kug, M. Lengaigne, M. J. McPhaden, K. Takahashi, A. Timmermann, G. Vecchi, M. Watanabe, and L. Wu, "Enso and greenhouse warming," Nature Climate Change **5**, 849–859 (2015).

[4] G. T. Rochelle, "Amine scrubbing for CO_2 capture," Science **325**, 1652–1654 (2009).

[5] A. C. Forse and P. J. Milner, "New chemistry for enhanced carbon capture: beyond ammonium carbamates," Chem. Sci. **12**, 508–516 (2021).

[6] S. Vasudevan, S. Farooq, I. A. Karimi, M. Saeys, M. C. Quah, and R. Agrawal, "Energy penalty estimates for co_2 capture: Comparison between fuel types and capture-combustion modes," Energy **103**, 709–714 (2016).

[7] J. H. Rheinhardt, P. Singh, P. Tarakeshwar, and D. A. Buttry, "Electrochemical capture and release of carbon dioxide," ACS Energy Letters **2**, 454–461 (2017).

[8] S. E. Renfrew, D. E. Starr, and P. Strasser, "Electrochemical approaches toward co2 capture and concentration," ACS Catalysis **10**, 13058–13074 (2020).

[9] I. Sullivan, A. Goryachev, I. A. Digdaya, X. Li, H. A. Atwater, D. A. Vermaas, and C. Xiang, "Coupling electrochemical co2 conversion with co2 capture," Nature Catalysis **4**, 952–958 (2021).

[10] R. Sharifian, R. M. Wagterveld, I. A. Digdaya, C. Xiang, and D. A. Vermaas, "Electrochemical carbon dioxide capture to close the carbon cycle," Energy Environ. Sci. **14**, 781–814 (2021).

[11] P. Scovazzo, J. Poshusta, D. DuBois, C. Koval, and R. Noble, "Electrochemical separation and concentration of ¡ 1carbon dioxide from nitrogen," Journal of The Electrochemical Society **150**, D91 (2003).

[12] D. H. Apaydin, E. D. Gowacki, E. Portenkirchner, and N. S. Sariciftci, "Direct electrochemical capture and release of carbon dioxide using an industrial organic pigment: Quinacridone," Angewandte Chemie International Edition **53**, 6819–6822 (2014).

[13] B. Gurkan, F. Simeon, and T. A. Hatton, "Quinone reduction in ionic liquids for electrochemical co2 separation," ACS Sustainable Chemistry & Engineering **3**, 1394–1405 (2015).

[14] Y. Liu, H.-Z. Ye, K. M. Diederichsen, T. V. Voorhis, and T. A. Hatton, "Electrochemically mediated carbon dioxide separation with quinone chemistry in salt-concentrated aqueous media," Nat Commun **11** (2020), 10.1038/s41467-020-16150-7.

[15] M. B. Mizen and M. S. Wrighton, "Reductive addition of CO_2 to 9,10phenanthrenequinone," J. Electrochem. Soc. **136**, 941 (1989).

[16] S. Voskian and T. A. Hatton, "Faradaic electro-swing reactive adsorption for co2 capture," Energy Environ. Sci. **12**, 3530–3547 (2019).

[17] Q. Li, C. Batchelor-McAuley, N. S. Lawrence, R. S. Hartshorne, and R. G. Compton, "Semiquinone intermediates in the two-electron reduction of quinones in aqueous media and their exceptionally high reactivity towards oxygen reduction," ChemPhysChem **12**, 1255–1257 (2011).

[18] T. Nagaoka, N. Nishii, K. Fujii, and K. Ogura, "Mechanisms of reductive addition of co2 to quinones in acetonitrile," Journal of Electroanalytical Chemistry **322**, 383–389 (1992), an International Journal Devoted to all Aspects of Electrode Kinetics, Interfacial Structure, Properties of Electrolytes, Colloid and Biological Electrochemistry.

[19] F. Simeon, M. C. Stern, K. M. Diederichsen, Y. Liu, H. J. Herzog, and T. A. Hatton, "Electrochemical and molecular assessment of quinones as co2-binding redox molecules for carbon capture," The Journal of Physical Chemistry C **126**, 1389–1399 (2022).

[20] J. E. Bachman, L. A. Curtiss, and R. S. Assary, "Investigation of the redox chemistry of anthraquinone derivatives using density functional theory," The Journal of Physical Chemistry A **118**, 8852–8860 (2014).

[21] Z. Wang, A. Li, L. Gou, J. Ren, and G. Zhai, "Computational electrochemistry study of derivatives of anthraquinone and phenanthraquinone analogues: the substitution effect," RSC Adv. **6**, 89827–89835 (2016).

[22] S. Schwan, D. Schrder, H. A. Wegner, J. Janek, and D. Mollenhauer, "Substituent pattern effects on the redox potentials of quinone-based active materials for aqueous redox flow batteries," ChemSusChem **13**, 5480–5488 (2020).

[23] S. Er, C. Suh, M. P. Marshak, and A. Aspuru-Guzik, "Computational design of molecules for an all-quinone redox flow battery," Chem. Sci. **6**, 885–893 (2015).

[24] D. D. Mndez-Hernndez, J. G. Gillmore, L. A. Montano, D. Gust, T. A. Moore, A. L. Moore, and V. Mujica, "Building and testing correlations for the estimation of one-electron reduction potentials of a diverse set of organic molecules," Journal of Physical Organic Chemistry **28**, 320–328 (2015).

[25] Q. Zhang, A. Khetan, and S. Er, "Comparison of computational chemistry methods for the discovery of quinone-based electroactive compounds for energy storage." Sci Rep **10** (2020), 10.1038/s41598-020-79153-w.

[26] W. Yin, A. Grimaud, I. Azcarate, C. Yang, and J.-M. Tarascon, "Electrochemical reduction of co2 mediated by quinone derivatives: Implication for lico2 battery," The Journal of Physical Chemistry C **122**, 6546–6554 (2018).

[27] T. Nagaoka, N. Nishii, K. Fujii, and K. Ogura, "Mechanisms of reductive addition of co2 to quinones in acetonitrile," Journal of Electroanalytical Chemistry **322**, 383–389 (1992).

[28] E. D. Glendening, C. R. Landis, and F. Weinhold, "Nbo 6.0: Natural bond orbital analysis program," Journal of Computational Chemistry **34**, 1429–1437 (2013).

[29] J. M. Galbraith and H. F. Schaefer, "Concerning the applicability of density functional methods to atomic and molecular negative ions," The Journal of Chemical Physics **105**, 862–864 (1996).

[30] H. B. Shore, J. H. Rose, and E. Zaremba, "Failure of the local exchange approximation in the evaluation of the h^- ground state," Phys. Rev. B **15**, 2858–2861 (1977).

[31] K. Schwarz, "Instability of stable negative ions in the xαmethod. a reply to a comment," Chemical Physics Letters **75**, 199–200 (1980).

[32] W. Koch and M. Holthausen, *A Chemist's Guide to Density Functional Theory* (Wiley, 2015).

[33] M. Brunavs, C. P. Dell, and W. Owton, "Direct fluorination of the anthraquinone nucleus: scope and application to the synthesis of novel rhein analogues," Journal of Fluorine Chemistry **68**, 201–203 (1994).

[34] O. Kaieda, K. Hirota, H. Itoh, M. Awashima, and T. Nakamura, "Method for production of fluorinated quinones," (1989).

[35] W. M. Owton, "Synthesis of 8-fluororhein," J. Chem. Soc., Perkin Trans. 1 , 2131–2135 (1994).

[36] Only the derivatives that give a bound $Q(CO_2)_2^{2-}$ structure by DFT are given.

[37] K. Wedege, E. Dražević, D. Konya, and A. Bentien, "Organic redox species in aqueous flow batteries: Redox potentials, chemical stability and solubility," Scientific Reports **6**, 39101 (2016).

[38] P. Singh, J. H. Rheinhardt, J. Z. Olson, P. Tarakeshwar, V. Mujica, and D. A. Buttry, "Electrochemical capture and release of carbon dioxide using a disulfidethiocarbonate redox cycle," Journal of the American Chemical Society **139**, 1033–1036 (2017), pMID: 28052189.

[39] J. Yang and J. Barlow, "Oxygen stable electrochemical co2 capture and concentration through alcohol additives," ChemRxiv (2021), 10.26434/chemrxiv-2021-2lg87.

[40] E. Epifanovsky, A. T. B. Gilbert, X. Feng, J. Lee, Y. Mao, N. Mardirossian, P. Pokhilko, A. F. White, M. P. Coons, A. L. Dempwolff, Z. Gan, D. Hait, P. R. Horn, L. D. Jacobson, I. Kaliman, J. Kussmann, A. W. Lange, K. U. Lao, D. S. Levine, J. Liu, S. C. McKenzie, A. F. Morrison, K. D. Nanda, F. Plasser, D. R. Rehn, M. L. Vidal, Z.-Q. You, Y. Zhu, B. Alam, B. J. Albrecht, A. Aldossary, E. Alguire, J. H. Andersen, V. Athavale, D. Barton, K. Begam, A. Behn, N. Bellonzi, Y. A. Bernard, E. J. Berquist, H. G. A. Burton, A. Carreras, K. Carter-Fenk, R. Chakraborty, A. D. Chien, K. D. Closser, V. Cofer-Shabica, S. Dasgupta, M. de Wergifosse, J. Deng, M. Diedenhofen, H. Do, S. Ehlert, P.-T. Fang, S. Fatehi, Q. Feng, T. Friedhoff, J. Gayvert, Q. Ge, G. Gidofalvi, M. Goldey, J. Gomes, C. E. Gonzlez-Espinoza, S. Gulania, A. O. Gunina, M. W. D. Hanson-Heine, P. H. P. Harbach, A. Hauser, M. F. Herbst, M. Hernndez Vera, M. Hodecker, Z. C. Holden, S. Houck, X. Huang, K. Hui, B. C. Huynh, M. Ivanov, . Jsz, H. Ji, H. Jiang, B. Kaduk, S. Khler, K. Khistyaev, J. Kim, G. Kis, P. Klunzinger, Z. Koczor-Benda, J. H. Koh, D. Kosenkov, L. Koulias, T. Kowalczyk, C. M. Krauter, K. Kue, A. Kunitsa, T. Kus, I. Ladjnszki, A. Landau, K. V. Lawler, D. Lefrancois, S. Lehtola, R. R. Li, Y.-P. Li, J. Liang, M. Liebenthal, H.-H. Lin, Y.-S. Lin, F. Liu, K.-Y. Liu, M. Loipersberger, A. Luenser, A. Manjanath, P. Manohar, E. Mansoor, S. F. Manzer, S.-P. Mao, A. V. Marenich, T. Markovich, S. Mason, S. A. Maurer, P. F. McLaughlin, M. F. S. J. Menger, J.-M. Mewes, S. A. Mewes, P. Morgante, J. W. Mullinax, K. J. Oosterbaan, G. Paran, A. C. Paul, S. K. Paul, F. Pavoevi, Z. Pei, S. Prager, E. I. Proynov, . Rk, E. Ramos-Cordoba, B. Rana, A. E. Rask, A. Rettig, R. M. Richard, F. Rob, E. Rossomme, T. Scheele, M. Scheurer, M. Schneider, N. Sergueev, S. M. Sharada, W. Skomorowski, D. W. Small, C. J. Stein, Y.-C. Su, E. J. Sundstrom, Z. Tao, J. Thirman, G. J. Tornai, T. Tsuchimochi, N. M. Tubman, S. P. Veccham, O. Vydrov, J. Wenzel, J. Witte, A. Yamada, K. Yao, S. Yeganeh, S. R. Yost, A. Zech, I. Y. Zhang, X. Zhang, Y. Zhang, D. Zuev, A. Aspuru-Guzik, A. T. Bell, N. A. Besley, K. B. Bravaya, B. R. Brooks, D. Casanova, J.-D. Chai, S. Coriani, C. J. Cramer, G. Cserey, A. E. DePrince, R. A. DiStasio, A. Dreuw, B. D. Dunietz, T. R. Furlani, W. A. Goddard, S. Hammes-Schiffer, T. Head-Gordon, W. J. Hehre, C.-P. Hsu, T.-C. Jagau, Y. Jung, A. Klamt, J. Kong, D. S. Lambrecht, W. Liang, N. J. Mayhall, C. W. McCurdy, J. B. Neaton, C. Ochsenfeld, J. A. Parkhill, R. Peverati, V. A. Rassolov, Y. Shao, L. V. Slipchenko, T. Stauch, R. P. Steele, J. E. Subotnik, A. J. W. Thom, A. Tkatchenko, D. G. Truhlar, T. Van Voorhis, T. A. Wesolowski, K. B. Whaley, H. L. Woodcock, P. M. Zimmerman,

S. Faraji, P. M. W. Gill, M. Head-Gordon, J. M. Herbert, and A. I. Krylov, "Software for the frontiers of quantum chemistry: An overview of developments in the q-chem 5 package," The Journal of Chemical Physics **155**, 084801 (2021).

[41] A. D. Becke, "Density functional thermochemistry. iii. the role of exact exchange," The Journal of Chemical Physics **98**, 5648–5652 (1993).

[42] C. Lee, W. Yang, and R. G. Parr, "Development of the colle-salvetti correlation-energy formula into a functional of the electron density," Phys. Rev. B **37**, 785–789 (1988).

[43] T. Clark, J. Chandrasekhar, G. W. Spitznagel, and P. V. R. Schleyer, "Efficient diffuse function-augmented basis sets for anion calculations. iii. the 3-21+g basis set for first-row elements, li-f," J. Comput. Chem. **4**, 294–301 (1983).

[44] R. Krishnan, J. S. Binkley, R. Seeger, and J. A. Pople, "Self-consistent molecular orbital methods. xx. a basis set for correlated wave functions," J. Chem. Phys. **72**, 650–654 (1980).

[45] A. V. Marenich, C. J. Cramer, and D. G. Truhlar, "Universal solvation model based on solute electron density and on a continuum model of the solvent defined by the bulk dielectric constant and atomic surface tensions," The Journal of Physical Chemistry B **113**, 6378–6396 (2009).

[46] A. V. Marenich, J. Ho, M. L. Coote, C. J. Cramer, and D. G. Truhlar, "Computational electrochemistry: prediction of liquid-phase reduction potentials," Phys. Chem. Chem. Phys. **16**, 15068–15106 (2014).

[47] K. Hernndez-Burgos, S. E. Burkhardt, G. G. Rodrguez-Calero, R. G. Hennig, and H. D. Abrua, "Theoretical studies of carbonyl-based organic molecules for energy storage applications: The heteroatom and substituent effect," The Journal of Physical Chemistry C **118**, 6046–6051 (2014).

[48] S. D. Pineda Flores, G. C. Martin-Noble, R. L. Phillips, and J. Schrier, "Bio-inspired electroactive organic molecules for aqueous redox flow batteries. 1. thiophenoquinones," The Journal of Physical Chemistry C **119**, 21800–21809 (2015).

FOR TABLE OF CONTENTS ONLY